Calcium- and BTB domain protein-modulated PINOID protein kinase directs polar auxin transport

Robert-Boisivon, H.S.

Chapter 2

TOUCHing PINOID: regulation of kinase activity by calcium-dependent sequestration

Hélène Robert[1], Carlos Samuel Galvan-Ampudia[1], Karen Sap, Remko Offringa

[1] These authors contributed equally to this manuscript

Abstract

Calcium is a broadly used second messenger in signaling pathways. For the specificity of its response, not only the spatio-temporal pattern, but also calcium "receptors" are essential. The signaling and polar transport of the plant hormone auxin are well-studied examples of processes modulated by calcium. PIN efflux carrier-driven auxin transport generates gradients and maxima that are essential for plant development. The Arabidopsis PINOID (PID) protein serine/threonine kinase has been identified as determinant in the polar subcellular targeting of PIN proteins, and thereby of the direction of transport. The finding that PID shows a calcium-dependent interaction with the calmodulin-related protein TOUCH3 (TCH3) provided the first molecular link between calcium and auxin transport. Here we show that TCH3 inhibits PID kinase activity by interacting with its catalytic domain, and we provide genetic evidence for the *in vivo* significance of this interaction. Furthermore, we show auxin-dependent sequestration of PID from the plasma membrane to the cytosol in protoplasts upon co-expression of TCH3. In root epidermal cells, where PID and TCH3 are co-expressed, auxin induces rapid and transient dissociation of PID from the plasma membrane away from its phospho-targets, the PIN proteins. This response requires the action of calmodulins and calcium channels. These results suggest that TCH3 is part of a feedback loop that modulates PIN polar targeting by rapid inhibition of PID activity in response to stimuli, such as auxin, that induce cytosolic calcium peaks.

Introduction

Calcium plays an important role as intracellular second messenger in a variety of signaling pathways. In plants, rapid changes in the cytosolic calcium concentration are required for the transduction of both abiotic signals and biotic stimuli (Bouché et al., 2005). In order to give an appropriate response, cells need to distinguish the calcium signals produced by these different stimuli. Spatial and temporal patterns of calcium responses, and also the presence of calcium "receptors" or sensors in the cell, are needed to give specificity to the signal (Luan et al., 2002, Sanders et al., 2002). These receptor proteins are able to monitor the changes in the calcium concentration by binding calcium through specific domains called EF hands (Strynadka and James, 1989). The conformational changes induced by binding of calcium to these proteins either induces their activation, or enhances their interaction with other proteins that are in turn activated or repressed (Travé et al., 1995, Luan et al., 2002, Sanders et al., 2002). Two main types of sensors are known: the calmodulins (CaMs) and the calcium-dependent protein kinases (CDPKs). CaMs are small proteins with typically four EF-hands without an effector domain. The transmission of the signal occurs through the interaction with a target enzyme to influence its activity (Snedden

and Fromm, 2001, Bouché et al., 2005). The CDPKs combine a calmodulin-like domain with a kinase domain. Binding of calcium directly activates the protein kinase (Cheng et al., 2002).

The phytohormone auxin regulates plant development by controlling basic cellular processes such as cell division, -differentiation and -elongation (Reinhardt et al., 2000, Nakajima and Benfey, 2002, Weijers and Jurgens, 2005). Several studies suggest that the auxin signaling pathway involves rapid changes in the cytosolic calcium concentration. For example, in wheat protoplasts (Shishova and Lindberg, 2004), maize coleoptile cells (Felle, 1988, Gehring et al., 1990a) and parsley cells (Gehring et al., 1990a), an increase of the cytosolic calcium concentration was detected within minutes after auxin application using calcium fluorescent dyes or ion-sensitive microelectrodes. The observation of an auxin-induced calcium pulse was not limited to protoplasts, but was also observed in intact plant tissues such as maize and pea roots (Gehring et al., 1990a).

Ever since the first observations of Darwin on the growth response of Canary grass coleoptiles to unidirectional light (Darwin, 1880), it is well-established now that auxin is transported from cell to cell in a polar fashion from its sites of synthesis to its sites of action (Muday and DeLong, 2001). This polar auxin transport (PAT) generates auxin gradients and maxima that mediate photo- and gravitropic growth responses, and are instructive for embryogenesis, meristem maintenance and organ positioning (Sabatini et al., 1999, Friml et al., 2002, Friml et al., 2003, Reinhardt et al., 2003). The mechanism of auxin transport has been widely studied, and PIN transmembrane proteins have been identified as auxin efflux carriers that direct this polar intercellular transport through their asymmetric subcellular localization (Morris et al., 2004, Petrášek et al., 2006, Wisniewska et al., 2006). The plant-specific AGC protein serine/threonine kinase PINOID (PID) was identified as a regulator of auxin transport and is the only determinant identified up to now in the polar targeting of PIN proteins. PID directs their localization at the apical (shoot facing) cell membrane, by phosphorylation of the PIN central hydrophilic loop (Benjamins et al., 2001, Friml et al., 2004, Michniewicz et al., 2007).

Calcium has also been implied as an important signal in the regulation of PAT in sunflower hypocotyls (Dela Fuente and Leopold, 1973), in gravistimulated roots (Lee and Evans, 1985) and in the phototropism signaling pathway. The light signal inducing phototropic growth is perceived by the PHOT1 blue receptor kinase. This induces a rapid increase in the cytoplasmic calcium concentration (Baum et al., 1999, Harada et al., 2003) and triggers a PIN-dependent auxin gradient. Auxin accumulation in the shaded side results in auxin-dependent transcriptions, leading to a shoot bending toward the light source (Friml et al., 2002, Esmon et al., 2006). The function of the rapid calcium response in phototropic growth and the downstream components of the signaling pathway are still uncharacterized.

Our previous finding that PID interacts in a calcium-dependent manner with the calcium-binding proteins PINOID BINDING PROTEIN1 (PBP1) and TOUCH3 (TCH3)

provided the first molecular evidence for calcium as a signal transducer in the regulation of auxin transport (Benjamins et al., 2003). TCH3 is a CaM-like protein containing 6 EF-hands, and its corresponding gene was initially identified as a touch-responsive gene (Braam and Davis, 1990, Sistrunk et al., 1994). Here we present a detailed study of the *in vivo* interaction between PID and TCH3. Using loss- and gain-of-function mutant lines, we confirm *in vitro* observations that TCH3 is a negative regulator of the PINOID kinase activity. This regulation occurs directly by inhibition of the kinase activity, as shown in phosphorylation assays, and by sequestration of PID from the plasma membrane where its phospho-targets are located (Michniewicz et al., 2007). Interestingly, auxin treatment also results in rapid transient re-localization of the membrane-associated kinase to the cytosol. We speculate that this occurs through its interaction with TCH3, which is enhanced by the auxin-induced increase in cytosolic calcium.

Results

TCH3 reduces the kinase activity by binding to the catalytic domain of PID

Previously we identified the calmodulin-like protein TCH3 as PID binding protein in a yeast two-hybrid screen. With *in vitro* pull-down assays we could show that the kinase-CaM interaction is calcium-dependent (Benjamins et al., 2003). In order to roughly map the TCH3 interaction site in PID, we incubated GST-tagged isolates of full-length PID, the N-terminal domain (aa 2-103), the catalytic domain (aa 75-398) or C-terminal domain (aa 339-438) with crude *E. coli* extracts containing Histidine (His)-tagged TCH3 (Figure 1A). Protein complexes were pulled down with glutathione beads and separated on gel. Western blot analysis using anti-His antibodies showed that TCH3 interacts with full-length PID or with its catalytic domain (Figure 1B, lanes 2 and 4) but not with the N- or C-terminal domains (Figure 1B, lanes 3 and 5) nor with GST alone (Figure 1B, lane 1). Binding to the catalytic domain suggested that TCH3 might affect PID kinase activity. Indeed, our previous studies showed that TCH3 reduces the *in vitro* phosphorylation activity of PID using traditional kinase assay with Myelin Basic Protein (MBP) as substrate (Benjamins et al., 2003). To confirm these results with a wider array of substrates, we incubated a commercial phospho-peptide chip with radiolabelled ATP and PID alone or in the presence of PBP1, a PID positive regulator (Benjamins et al., 2003), or of both PBP1 and TCH3. For a quantitative comparison of the differences in PID activity, we focused on the phosphorylation intensity of four peptides, one of which represented a phospho-target in MBP. PID efficiently phosphorylated all four peptides (Figures 2A and 2D) and in presence of PBP1, the phosphorylation intensity was significantly increased (Figures 2B and 2D) which corroborated the role of PBP1 as positive regulator of PID (Benjamins et al., 2003). When TCH3 was added to the last mix, the phosphorylation intensity was significantly

reduced to even below the basal level of PID alone (Figures 2C and 2D). These data corroborate our previous data that TCH3 is a negative regulator of PID kinase activity *in vitro* and indicate that TCH3 binding to PID is able to overrule this positive effect of PBP1.

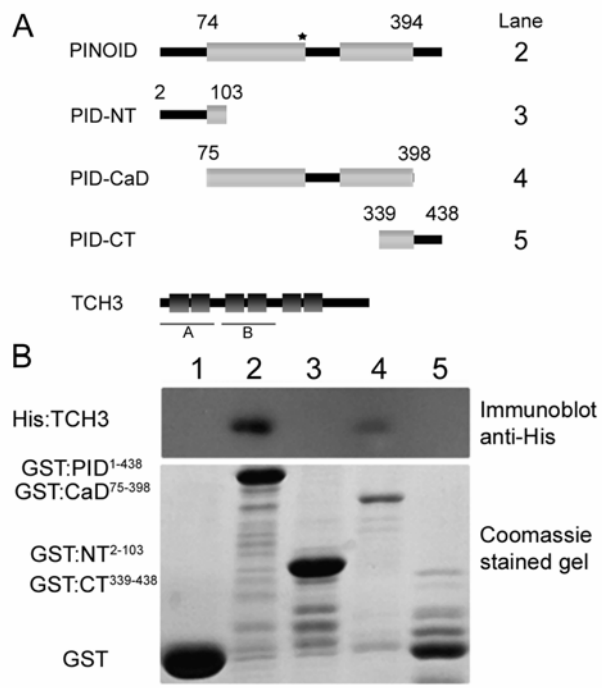

Figure 1. TCH3 interacts with the catalytic domain of PID.
(A) A schematic representation of the proteins used in the *in vitro* pull-down assay. Full-length PID (498 aa) and its deletion mutants: the N-terminal portion (PID-NT, aa 2-103), the catalytic domain (PID-CaD, aa 75-398) and the C-terminal portion (PID-CT, aa 339-438), are shown. The light grey boxes represent the PID catalytic domain (aa 74-394), comprising 11 conserved sub-domains and the amino acid insertion between sub-domain VII and VIII (aa 226-281). The star indicates the DFG to DFD mutation characteristic for the plant-specific AGCVIII protein kinases. The numbers indicated on the right correspond to the lane numbers of the Western blot in (B). TCH3 (324 aa) is depicted with the six EF-hand domains (aa 12-38, 50-74, 101-127, 139-163, 191-217, 228-253) as dark grey boxes. The lines A and B represent the perfect tandem repeat comprising EF-hands pairs 1-2 and 3-4.
(B) Western blot analysis (top) with anti-His antibodies detects His-tagged TCH3 after pull-down with GST-tagged PID (lane 2) or GST-tagged PID catalytic domain (GST:CaD, lane 4), but not after pull-down with GST-tagged PID N-terminal (GST:NT, lane 3) or C-terminal (GST:CT, lane 5) domains or with GST alone (lane 1). Coomassie stained gel (bottom) showing the input of proteins used in the pull-down assay.

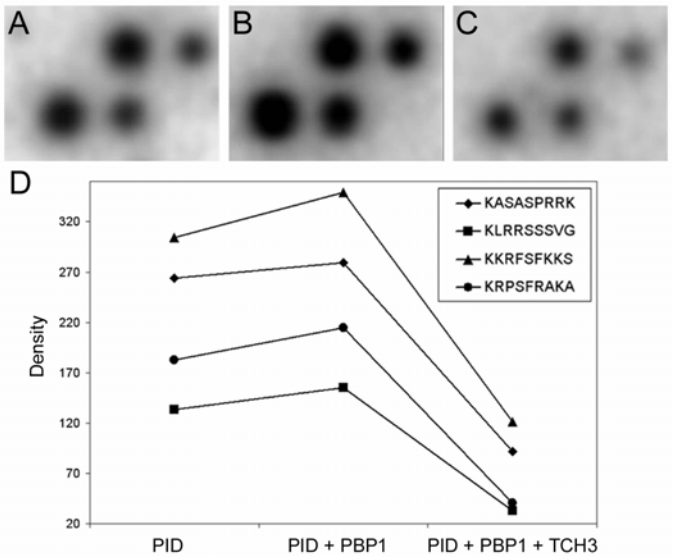

Figure 2. TCH3 reduces PID kinase activity *in vitro.*
(A-C) Kinase assay using a chip where PID alone (A), PID and the positive regulator PBP1 (B), or PID, PBP1 and TCH3 (C) were incubated with radiolabelled ATP.
(D) Quantification of the phosphorylation density of the four peptides shown in (A-C) confirms that TCH3 represses PID kinase activity *in vitro*.

TCH3 *overexpression lines and* **tch3** *loss-of-function mutants do not show phenotypes*

To further analyze the possible function of TCH3 as a regulator of the PID pathway *in planta*, we obtained the mutant alleles *tch3-2* and *tch3-1* from the SALK collection with a T-DNA inserted at respectively positions -134 and -120 relative to the ATG of *TCH3.* Northern blot analysis indicated that *tch3-2* was a null allele, whereas in *tch3-1* the expression was enhanced (Figure 3A). Another SALK line with a T-DNA insertion at position -71, named *tch3-3*, was found to be a complete knock-out both on Northern and Western blots (J. Braam, pers. com.). Both *tch3-2* and *tch3-3* (J. Braam, pers. com.) alleles did not show any obvious phenotypes, suggesting that TCH3 is functionally redundant with the most related calmodulin-like proteins CaML9 and CML10 (McCormack and Braam, 2003).

In order to generate gain-of-function alleles, *TCH3* full-length cDNA was overexpressed in Arabidopsis Columbia under the strong *35S* promoter. Despite high expression levels in four independent single locus insertion lines (Figure 3B), no obvious phenotypes were observed in the *35S::TCH3* plants. Our analysis focused on auxin-related phenotypes (gravitropic growth, sensitivity to IAA and NPA and lateral root development) and we may have therefore missed phenotypes related to the touch response pathway.

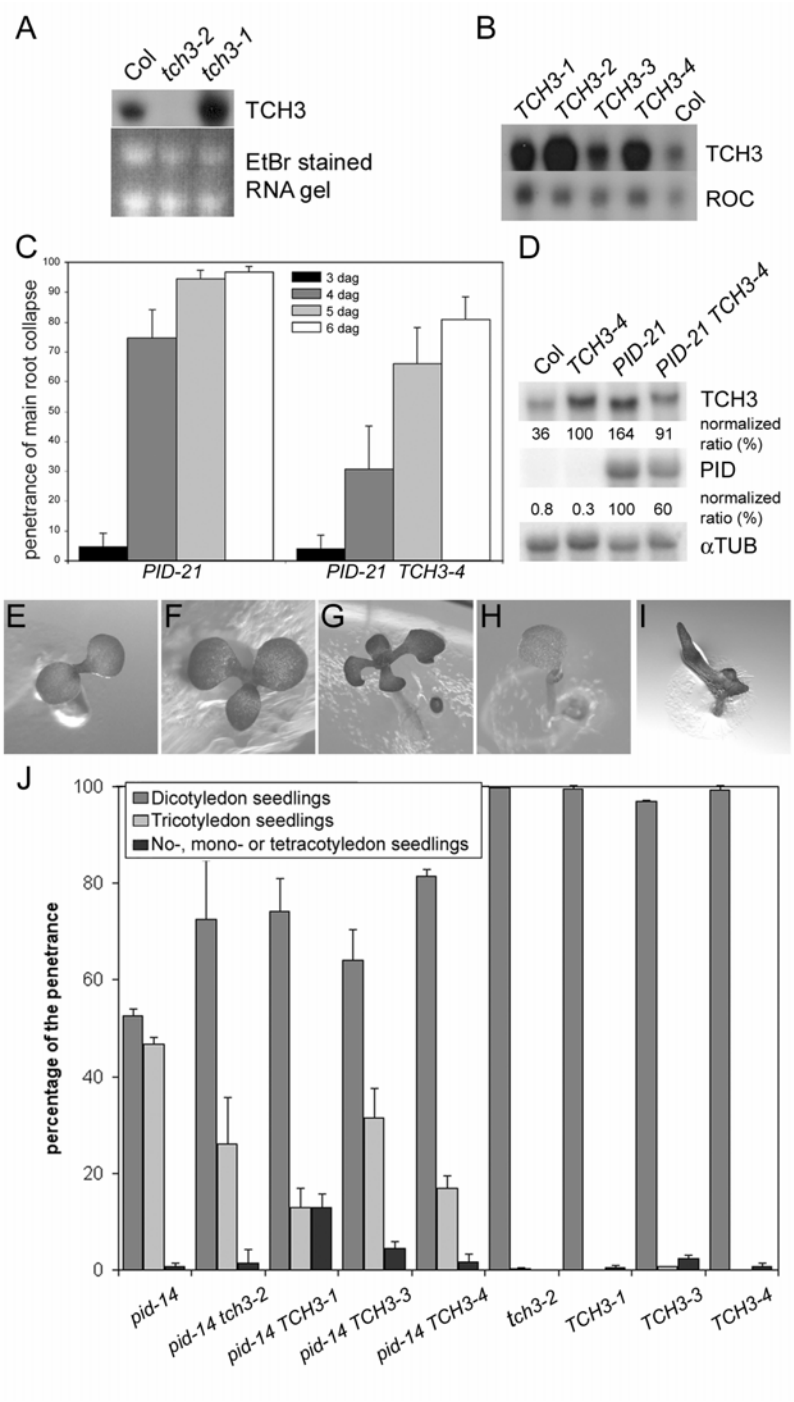
A
Col
tch3-2
tch3-1
TCH3
EtBr stained
RNA gel
B
TCH3-1
TCH3-2
TCH3-3
TCH3-4
Col
TCH3
ROC
C
penetrance of main root collapse
3 dag
4 dag
5 dag
6 dag
PID-21
PID-21 TCH3-4
D
Col
TCH3-4
PID-21
PID-21 TCH3-4
TCH3
36 100 164 91
normalized ratio (%)
PID
0.8 0.3 100 60
normalized ratio (%)
αTUB
E
F
G
H
I
J
percentage of the penetrance
Dicotyledon seedlings
Tricotyledon seedlings
No-, mono- or tetracotyledon seedlings
pid-14
pid-14 tch3-2
pid-14 TCH3-1
pid-14 TCH3-3
pid-14 TCH3-4
tch3-2
TCH3-1
TCH3-3
TCH3-4

Figure 3: TCH3 is a negative regulator of PID *in vivo.*
(A) Northern blot showing *TCH3* expression in *tch3-2* (SALK_090554) and *tch3-1* (SALK_056345), having T-DNA insertions at respectively position -140 and -120 relative to the ATG of the *TCH3* gene: *tch3-2* shows no detectable mRNA expression, whereas the expression in *tch3-1* is enhanced. An Ethidium bromide stained RNA gel is shown to compare loading.
(B) Northern blot showing the level of *TCH3* overexpression in four independent transgenic lines carrying the *35Spro:TCH3* construct. The blot was first hybridized with the *TCH3* cDNA (top), and subsequently stripped and hybridized with the *ROC* cDNA to show the loading (bottom).
(C) The percentage of the main root meristem collapse in the *35Spro:PID-21* and in *35Spro:PID-21 35Spro:TCH3-4* lines. When *TCH3* is overexpressed the root meristem collapse is significantly delayed (Student's t-test, $p < 0.05$).
(D) Northern blot analysis showing the expression level of *TCH3* (top), *PID* (middle) and *αTubulin* (bottom) in seedlings of the lines used in (C). The same blot was successively hybridized with the *PID*, *TCH3* and *αTubulin* cDNA. Intensities were quantified using ImageQuant and normalized to the corresponding *αTubulin* sample to compensate for loading differences. The sample with *TCH3* or *PID* overexpression alone was put at 100%.
(E-I) Observed seedling phenotypes, ranging from di- (E) and tri-cotyledon seedlings (F) as seen in the *pid-14* allele, to tetra- (G), mono- (H) and no-cotyledon seedlings (I) as seen in the *pid-14 tch3-2*, and *pid-14 35Spro:TCH3* lines.
(J) The percentage of the penetrance of the aberrant number of cotyledons was analyzed in seedling population of *pid-14/+*, *pid-14/+ tch3-2*, *pid-14/+ 35Spro:TCH3-1*, *pid-14/+ 35Spro:TCH3-3*, *pid-14/+ 35Spro:TCH3-4*.

TCH3 *overexpression reduces* PID *gain-of-function root meristem collapse*

The above data suggest that TCH3 provides feedback regulation on the PID kinase activity, in response to auxin or other signals that induce rapid changes in the cytosolic calcium concentration. As both loss-of-function and gain-of-function lines did not provide further information, we crossed the *TCH3* overexpression line *35Spro:TCH3-4* with the overexpression line *35Spro:PID-21*. High *PID* expression in the root causes the collapse of the main root meristem, which is triggered by the lack of an auxin maximum due to the basal-to-apical PIN polarity switch (Benjamins et al., 2001, Friml et al., 2004). This phenotype is observed in only 5 % of the seedlings at 3 days after germination (dag), but has occurred in up to 97 % of the seedlings at 6 dag (Figure 3C). Overexpression of *TCH3* significantly reduced the root meristem collapse (Figure 3C) from 75 % to 31 % at 4 dag (Student's t-test, $p < 0.05$) and from 97 % to 81 % at 6 dag (Student's t-test, $p = 0.06$). The levels of *PID* and *TCH3* expression were slightly lower in 5 days old *35Spro:PID-21 35Spro:TCH3-4* seedlings than in *35Spro:PID-21* and *35Spro:TCH3-4* seedlings (Figure 3D), but not enough to explain the difference in timing of the root meristem collapse phenotype between *35Spro:PID-21* and *35Spro:PID-21 35Spro:TCH3-4*. These observations corroborate the proposed role of TCH3 as negative regulator of PID kinase activity (above and (Benjamins et al., 2003).

pid *loss-of-function mutant is sensitized to changes in* TCH3 *expression*

Loss-of-function *pid* alleles have a characteristic defect in embryo development mostly leading to seedlings with three cotyledons. The penetrance of this phenotype varies between

10 and 50 % depending on the strength of the mutant allele (Bennett et al., 1995, Christensen et al., 2000, Benjamins et al., 2001). In the *pid-14* allele, 46 % of the homozygous seedlings have three cotyledons (Figures 3F and 3J) and less than 1 % develops a single cotyledon (Figures 3H and 3J). To investigate the influence of TCH3 on the *pid* embryo phenotype, the *tch3-2* allele and the *35Spro:TCH3-1*, *-3* and *-4* overexpression lines were crossed with *pid-14*, and progeny homozygous for the *tch3-2* loss-of-function or the *35Spro:TCH3* gain-of-function locus and segregating for the *pid-14* allele were scored for cotyledon defects. The percentages were calculated relative to the expected number of *pid-14* homozygous individuals. The *tch3-2* loss-of-function allele did not show aberrant cotyledon phenotypes and in the three *TCH3* overexpressing lines only a low percentage of monocotyledon seedlings was observed (up to 2 % for *35Spro:TCH3-3*, Figure 3J). In all the double mutant lines, the overall penetrance of aberrant cotyledon phenotypes was reduced (17 to 31 % for the double mutants versus 46 % for *pid-14*, Figure 3J), whereas a significantly higher number of seedlings showed stronger cotyledon defects, such as four cotyledons (< 1 % for *pid-14 35Spro:TCH3-4*, Figure 3G), one cotyledon (ranging from 2 % for *pid-14 tch3-2* and *pid-14 35Spro:TCH3-4*, up to 10 % for *pid-14 35Spro:TCH3-1*, Figure 3H) or even no cotyledons (3 % for *pid-14 35Spro:TCH3-1*, Figure 3I). Although there is a clear effect of both *TCH3* overexpression and loss-of-function on the severity of the *pid* loss-of-function seedling phenotypes, the data do not indicate a clear negative regulatory function for TCH3, as observed in the *in vitro* phosphorylation assays or for the PID overexpression-induced root meristem collapse phenotype. No correlation between the level of *TCH3* overexpression and the increase in number of mono-, no- and tetracotyledon seedlings is found. Possibly, during embryo development, a critical balance between the cellular PID activity and TCH3 levels is required for proper cotyledon positioning, and both *TCH3* overexpression and loss-of-function can disturb this balance, as indicated by the significant number of seedlings with defects in cotyledon positioning. The fact that the *pid* loss-of-function mutant background is sensitized to changes in *TCH3* expression, corroborates the functional relationship between PID and TCH3.

TCH3 mediates auxin-dependent sequestration of PID from the plasma membrane

The subcellular localization of TCH3 was tested by transfecting Arabidopsis protoplasts with a *35Spro:TCH3:YFP* construct. The TCH3:YFP fusion protein was found to be cytoplasmic (Figure 4A), overlapping with soluble CFP (Figures 4B and 4C). In contrast to soluble CFP (Figure 4B), however, TCH3:YFP was excluded from the nucleus (Figures 4B and 4C). This localization differed significantly from that of PID, which is membrane-associated both in protoplasts (Figure 4E), or *in planta* (Figure 6E) (Lee and Cho, 2006, Michniewicz et al., 2007).

When *35Spro:PID:CFP* and *35Spro:TCH3:YFP* were co-transfected in auxin-starved Arabidopsis protoplasts, PID:CFP and TCH3:YFP did not co-localize and remained

at their respective subcellular location, the plasma membrane and the cytoplasm (Figures 4F-H). Interestingly, when cells were cultured in normal auxin-containing medium, PID subcellular localization became cytoplasmic in presence of TCH3 (Figures 4I-K), suggesting that the auxin-dependent interaction with TCH3 sequesters PID from the plasma membrane. The fact that auxin treatment of auxin-starved protoplasts does not lead to PID sequestration when TCH3 is co-transfected (results not shown), suggests that protoplasts are desensitized to auxin, and that the sequestration observed in auxin grown protoplasts is probably the result of PID and TCH3 overexpression and constitutively elevated calcium levels.

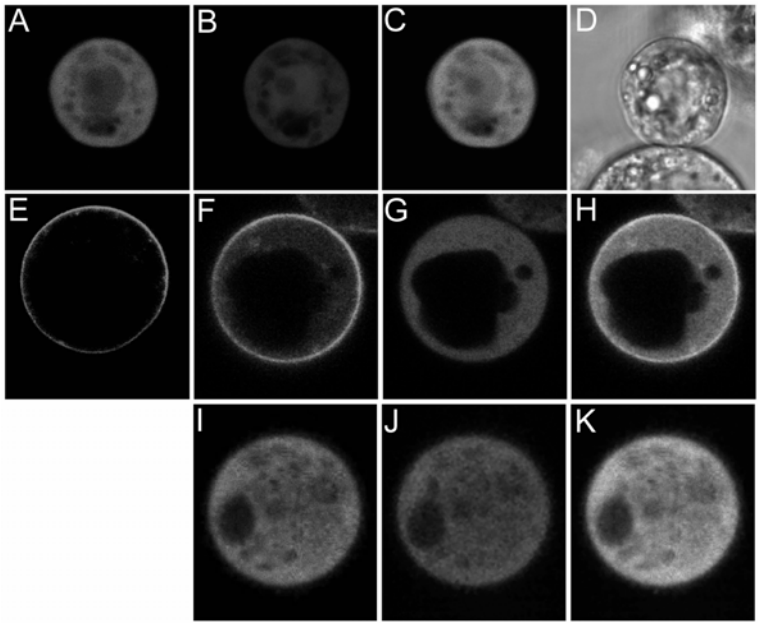

Figure 4. TCH3 and PID co-localization is auxin-dependent.
(A-D) *35Spro:TCH3:YFP* was co-transfected with *35Spro:CFP* in Arabidopsis protoplasts. Comparison of the YPF image (A) with the CFP image (B) or the merged image (C) indicates that TCH3 is cytoplasmic and excluded from the nucleus. (D) A transmitted light image of the protoplast in (A-C).
(E) Arabidopsis cell suspension protoplast transfected with *35Spro:PID:CFP* shows a plasma membrane localization.
(F-K) Auxin-starved (F-H) or auxin-cultured (I-K) Arabidopsis protoplasts co-transfected with *35pro:PID:CFP* and *35Spro:TCH3:YFP*. Shown are the CFP channel (F, I), the YFP channel (G, J) or the merged image (H, K). PID is membrane localized in auxin-starved protoplasts but co-localizes with TCH3 in the cytoplasm when cells are cultured in presence of auxin.

A

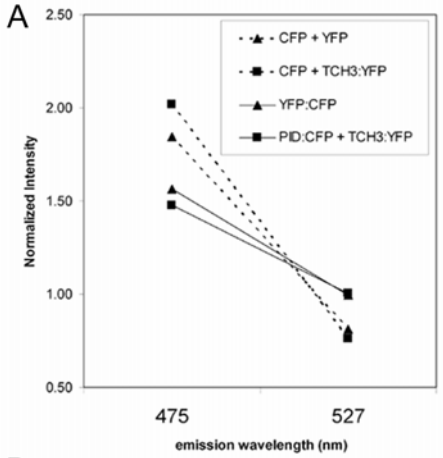

B

		Student T test p<0.05	
	Slope	475 nm	527 nm
CFP + YFP	-0.020		
CFP + TCH3:YFP	-0.024	0.394	0.515
YFP:CFP	-0.011	0.046	0.016
PID:CFP + TCH3:YFP	-0.009	0.040	0.036

Figure 5. TCH3 interacts with PID *in vivo.*
(A) Graph showing the fluorescence intensities at 475 nm (CFP emission peak) and 527 nm (YFP emission peak) during lambda scanning using an excitation wavelength of 457 nm (donor, CFP) in Arabidopsis protoplasts expressing a translational fusion between YFP and CFP (triangle, plain line, positive control), or co-expressing PID:CFP and TCH3:YFP (square, plain line), CFP and TCH3:YFP (square, dotted line, negative control) or CFP and YFP (triangle, dotted line, negative control). The observed quenched intensities at the CFP emission peak and enhanced intensities at the YFP emission peak of the PID:CFP-TCH3:YFP sample are indicative for FRET, and corroborate the *in vivo* interaction between TCH3 and PID.
(B) Table indicating the slope of the curves shown in (A) and the *P*-values of Student's t-tests, in which the 475 nm (CFP) and the 527 nm (YFP) emission intensities of CFP and TCH3:YFP, and YFP:CFP were compared with those of YFP and CFP expressing protoplasts; and of PID:CFP and TCH3:YFP compared with those of TCH3:YFP and 35Spro:CFP.

To confirm the *in vivo* interaction between the two proteins, we checked for the presence of Förster (Fluorescence) Resonance Energy Transfer (FRET) between the CFP and YFP moieties of the co-expressed fusion proteins using confocal lambda scanning (Siegel et al., 2000). No bleed-through occurred in protoplasts co-expressing with CFP and YFP, meaning that YFP was not excited by CFP excitation wavelength (457 nm) and vice versa (data not shown). However, excitation with 457 nm leads to a significant CFP-derived signal at the YFP emission wavelength (527 nm). FRET in the test sample is therefore signified by a quenched signal at the CFP emission wavelength (475 nm) and higher signal at the YFP emission wavelength (527 nm), as compared to control transfections with non-interacting versions of CFP and YFP (*35Spro:CFP* co-transfected either with *35Spro:TCH3:YFP* or with *35Spro:YFP*). Indeed, a significant FRET signal could be detected in protoplast that co-expressed TCH3:YFP and PID:CFP. The lambda scanning profile matched that of protoplasts expressing the YFP:CFP fusion protein for which FRET is expected (Figures 5A and 5B). These data corroborate our earlier hypothesis that TCH3 sequesters PID from the plasma membrane to the cytoplasm by interaction with the protein kinase.

Auxin-induced calcium-dependent sequestration of PID in root epidermal cells

Previous studies (Sistrunk et al., 1994, Antosiewicz et al., 1995, Benjamins et al., 2001) already indicated that expression patterns of *PID* and *TCH3* overlap to allow a functional *in vivo* interaction between the two proteins. As shown by a *TCH3pro:TCH3:GUS* translation fusion, *TCH3* is expressed in epidermis cells of the elongation zone of the root tip (Figure 6A), in the vasculature of the root at the root-hypocotyl junction (Figure 6B), in the vasculature and in the stomata of leaves and cotyledons (Figure 6C), and at the shoot apical meristem (Figure 6C). As the expression of *TCH3* is auxin responsive, it preferentially accumulates in cells that are part of auxin response maxima, e.g., in the shoot apical meristem and root columella, in vascular tissues in roots, leaves and sepals and in the anthers and stigmas of flowers (Sistrunk et al., 1994, Antosiewicz et al., 1995). Upon IAA treatment, *TCH3* expression is strongly induced in the root, where it is extended to the vasculature and the epidermis of the complete root (Figure 6D). *PID* is also auxin responsive and is co-expressed with *TCH3* in the epidermis cells in the elongation zone of the root tip, in the shoot apical meristem and in flowers (Benjamins et al., 2001), suggesting a functional interaction between the two proteins in these tissues.

To investigate the biological relevance of the auxin-dependent, TCH3-mediated sequestration of PID observed in protoplasts, we used the *PIDpro:PID:VENUS* line (Michniewicz et al., 2007) to study the dynamics of the subcellular localization of PID in wild type Arabidopsis and *35Spro:TCH3* overexpression epidermis root cells. In both backgrounds, PID localized at the membrane (Figures 6E and 6M) (Lee and Cho, 2006, Michniewicz et al., 2007), suggesting that overexpression of *TCH3* alone is not sufficient to trigger the change in PID subcellular localization *in planta*. Upon auxin treatment, however, PID was rapidly released in the cytoplasm within 5 minutes of treatment (Figure 6F), and plasma membrane localization was restored 10 minutes after auxin addition (Figures 6G-J). Pre-treatment of seedlings with tetracain (Tc), a calmodulin inhibitor, or lanthanum (La), a calcium channel blocker, did not influence the PID localization by itself (Figures 6K and 6S), but did inhibit IAA-induced dissociation of PID from the plasma membrane (Figures 6L and 6T). PID localization was not influenced by TCH3 overexpression. These data suggest that this dissociation is dependent on an increase in the cytoplasmic calcium concentration involving plasma membrane calcium channels, and that this calcium signal is translated by one or more CaMs. In view of our results in protoplasts, it is likely that the CaM-like protein TCH3 is involved in this process.

Together the results described here suggest that TCH3 acts as a calcium receptor in the PID signaling pathway that translates rapid peaks in cytosolic calcium into subtle changes in PIN polarity, by influencing the activity and by sequestering the kinase from the plasma membrane to the cytoplasm.

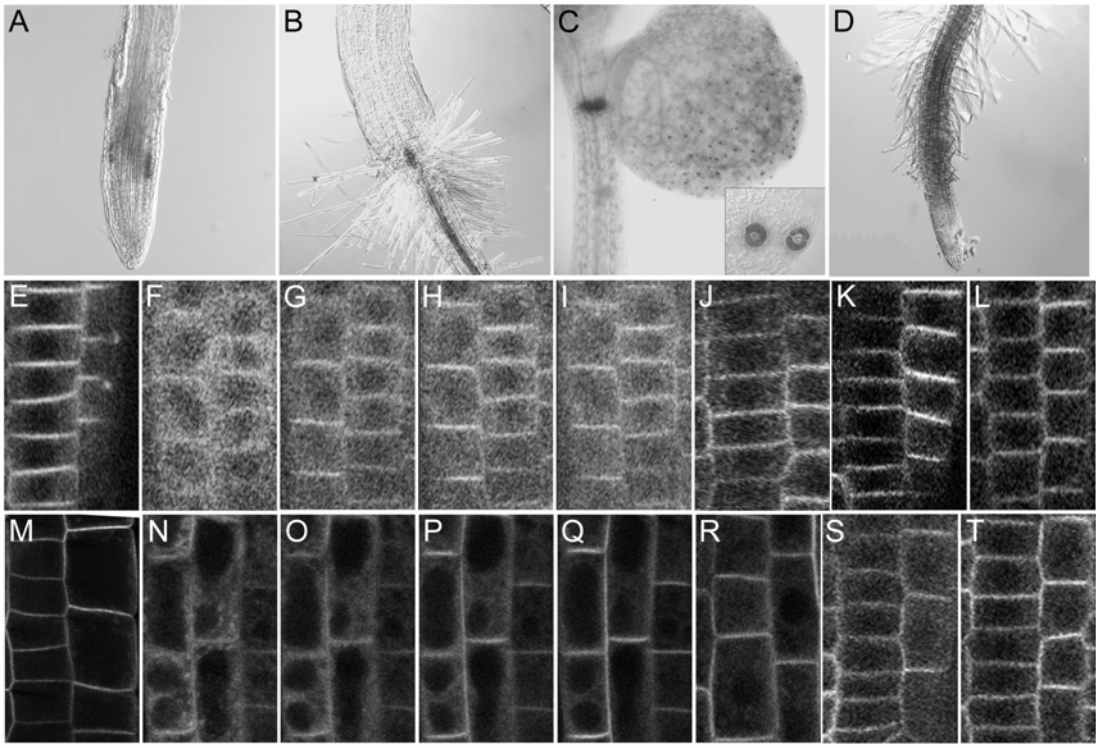

Figure 6. TCH3 and auxin cause PID to dissociate from the plasma membrane.
(A-D) Histochemical staining of *TCH3pro:TCH3:GUS* seedlings (Sistrunk et al., 1994) showing that *TCH3* is expressed in epidermis cells of the elongation zone of the root tip (A), in vascular tissues at the root-hypocotyl junction (B), in the shoot apical meristem and in vascular tissues and stomata (inset) of the cotyledon (C). *TCH3* expression in roots is enhanced when grown on 0.1μM IAA (D).
(E) PID is membrane localized in *PIDpro:PID:VENUS* epidermal cells of seedling root tips.
(F-J) PID transiently dissociates from the plasma membrane 5 min after IAA treatment (F), but rapidly returns to the plasma membrane (10 min (G), 20min (H), 30 min (I) and 1 h (J) treatment).
(K-L, S-T) Pre-treatment with tetracain (30 min incubation, K-L), a CaM inhibitor, or Lanthanum (30 min incubation, S-T), a calcium channel inhibitor, does not influence PID localization (K, S) but blocks the auxin-induced dissociation of PID from the plasma membrane (5 min treatment with IAA and inhibitors, L, T).
(M-R) PID shows normal plasma membrane localization (M) and IAA-induced transient dissociation from the plasma membrane (5min (N), 10min (O), 20 min (P), 30 min (Q), 1h (R)) in seedling root tips of the *PIDpro:PID:YFP 35Spro:TCH3-2* line.

Discussion

Calcium is a common second messenger in signaling pathways, and has been found as one of the early signals in auxin responses. Experiments on plant cells showed that the cytosolic calcium concentration is increased within few minutes after auxin application (Felle, 1988,

Gehring et al., 1990a, Shishova and Lindberg, 2004). Furthermore polar auxin transport (PAT) is suppressed by application of the calcium chelator EDTA, and restored after application of a calcium solution (Dela Fuente and Leopold, 1973) indicating that calcium is also an important second messenger in the regulation of auxin transport.

PIN proteins are components of the cellular auxin efflux machinery. Their subcellular localization determines the direction of the auxin transport (Wisniewska et al., 2006, Petrášek et al., 2006). The protein serine/threonine kinase PINOID regulates PAT by establishing the proper apico-basal polarity of the PIN auxin efflux carriers (Friml et al., 2004). The finding that two calcium binding proteins PBP1 and TCH3 interact with PID to regulate its kinase activity *in vitro*, provided a first molecular link between calcium and the regulation of PAT (Benjamins et al., 2003). Here we investigated the *in vivo* role of TCH3 in the PID signaling pathway. First, we identified that TCH3 binds the catalytic domain of the PID kinase, and used *in vitro* kinase assays and genetic analysis to confirm the previous observations that TCH3 is a regulator of PID kinase activity (Benjamins et al., 2003). Next, we showed the co-localization and the interaction between TCH3 and PID in Arabidopsis protoplasts. Finally, we could demonstrate that TCH3 is involved in PID subcellular localization dynamics, clarifying the molecular link between calcium signaling and auxin transport.

TOUCHing PID: a regulatory loop that translates cellular calcium levels to PIN polarity

Previously, we used *in vitro* pull down assays to show that TCH3 interacts with PID in a calcium-dependent manner (Benjamins et al., 2003). Here, a similar assay was used in combination with PID deletion constructs to show that TCH3 interacts with the PID catalytic domain. Moreover, co-expression of TCH3 and PID in Arabidopsis protoplasts and subsequent FRET measurements demonstrated the *in vivo* interaction between the two proteins, and showed that TCH3 sequesters the normally plasma membrane-associated PID kinase to the cytoplasm. This suggests that interaction with TCH3 with the catalytic domain of PID provokes the release of the kinase from the plasma membrane. The cytoplasmic PID sequestration is auxin-dependent, as auxin-starved protoplasts do not show internalization of PID. Most likely, auxin treatment of protoplasts results in elevated levels of cytosolic calcium, which in turn enhances the affinity of the TCH3 CaM-like protein for PID.

Recent data by Zegzouti and co-workers indicated that PID binds to phosphorylated inositides and phosphatidic acid, and that the amino acid insertion in the PID catalytic domain (insertion domain) is the key determinant in membrane association of the kinase (Zegzouti et al., 2006). We therefore hypothesize that PID co-localizes at the plasma membrane with its phosphorylation targets, the PIN auxin efflux carriers (Michniewicz et al., 2007), through direct binding of membrane components to the insertion domain. An increase in cytosolic calcium, e.g. induced by auxin, facilitates

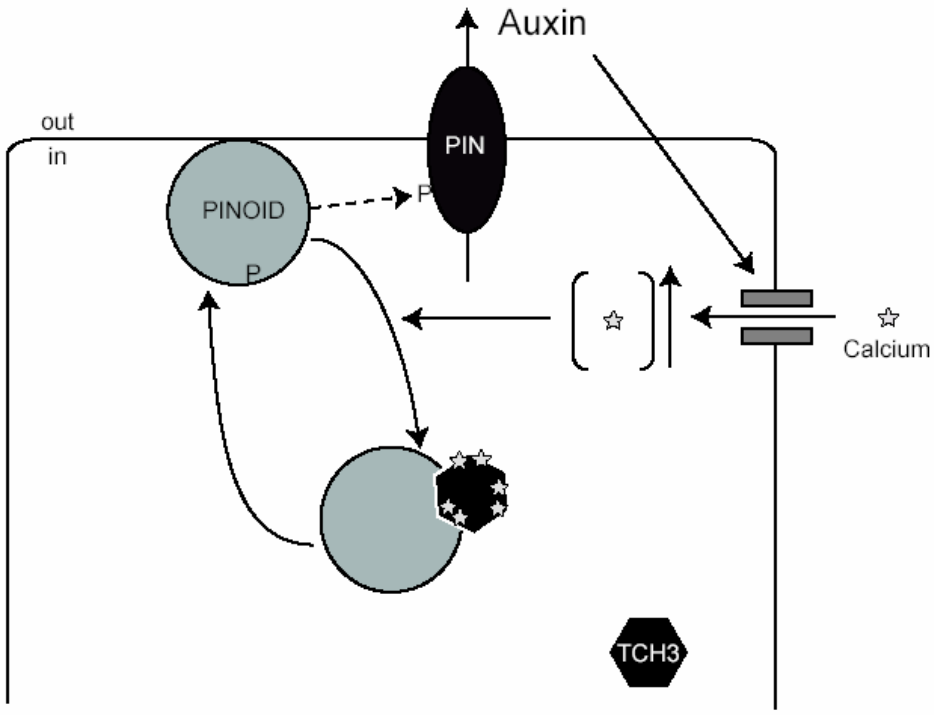

Figure 7. PID activity and subcellular localization is mediated by calcium and the calcium-binding proteins TCH3.
PID is a plasma membrane-associated protein kinase in proximity of its phospho-targets, the PIN auxin efflux carriers. Low calcium levels stabilize membrane association PID activity. Increases in calcium concentrations, via calcium channels in the plasma membrane, for example in response to elevated auxin levels, stimulate the interaction with the calmodulin-like TCH3, and this inhibits PID activity and triggers the dissociation of PID from the plasma membrane. P: phosphate group from a phosphorylation event, stripped line: phosphorylation reaction, plain line: signaling events, stars: calcium.

binding of TCH3 to the catalytic domain of PID, thereby preventing the kinase-lipid interaction and resulting in sequestration of the kinase away from its phospho-targets to the cytoplasm (Figure 7). Based on this model, it would be interesting to test whether TCH3 and phosphoinositides are competing for the interaction with the PID catalytic domain.

PKC, one of the animal orthologs of the plant specific AGCVIII kinases to which PID belongs (Galván-Ampudia and Offringa, 2007) directly binds calcium through a C2 domain. Calcium binding to this domain promotes a change in PKC subcellular localization from the cytosol to the plasma membrane and enhances the affinity of the C2 domain for phosphorylated inositides (Corbálan-Garcia et al., 2007). This plasma membrane translocation activates the PKC kinase. PID is also thought to be active at the plasma membrane. However in this case the (auxin-induced) increase in cytosolic calcium levels

results in the opposite effect and removes the kinase from the plasma membrane. PID does not have the typical calcium binding domains, and instead the kinase has evolved to interact in a calcium-dependent manner with calcium receptors, such as TCH3. Changes in subcellular localization are commonly used cellular mechanism to regulate protein activity by sequestering proteins away from their targets. To our knowledge, the calcium- and CaM-dependent release of the PID kinase is a new form of regulating the activity of a kinase that steers the polar subcellular targeting of transporter proteins.

TCH3: part of feedback loop of auxin on the direction of its own transport?

The proposed model in Figure 7 implies that a calcium release negatively and transiently regulates PID activity through its TCH3-induced dissociation from the plasma membrane, away from its phospho-targets, the PIN proteins. This TCH3-dependent inactivation of PID may be part of a regulatory loop that allows fast and possibly subtle alterations in PIN polarity in response to signals that lead to rapid changes in cytosolic calcium levels, such as auxin (Felle, 1988, Gehring et al., 1990a, Shishova and Lindberg, 2004), unidirectional blue light or gravity (Lee and Evans, 1985, Gehring et al., 1990b, Baum et al., 1999, Harada et al., 2003). Auxin is known to regulate its own transport, firstly by inhibiting PIN endocytosis (Paciorek et al., 2005), and secondly by regulating the subcellular PIN localization in Arabidopsis roots (Sauer et al., 2006), probably in order to canalize and increase the auxin flow in response to increased cellular auxin concentrations. Sauer and co-workers concluded that PID is not required for auxin-dependent PIN lateralization in root cells, because they still observed PIN lateralization in auxin-treated *35Spro:PID* seedlings (Sauer et al., 2006).

Auxin-induced PIN lateralization involves TIR1-dependent induction of auxin responsive gene expression, and does not occur as rapid as the auxin-induced dissociation of PID from the membrane that we report here. Our results suggest that elevated cellular auxin levels may transiently alter PID kinase activity by subcellular localization changes and inhibition of its kinase activity via TCH3 interaction. This may set the stage for the auxin-dependent PIN lateralization, or may only lead to a subtle modulation of PIN polar targeting. The fact that none of *TCH3* loss- and gain-of-function mutants display obvious phenotypes, and that we have not been able to detect changes in PIN polar targeting in roots of *35Spro:TCH3* and *tch3* mutant lines (M. Sauer, unpublished results) nor in *pid* knock-out roots (Friml et al., 2004), may be explained by calcium dependency of the PID-TCH3 interaction (*35Spro:TCH3*) and by functional redundancy with other CaMs (*tch3*) or with the PID-related kinases (*pid*).

Material and methods

Molecular cloning and constructs

Molecular cloning was performed following standard procedures (Sambrook et al., 1989). Bacteria were grown on LC medium containing 100 µg/ml carbenicillin (Cb, all high copy plasmids), 50 µg/ml kanamycin (Km, pGreen) or 250 µg/ml spectinomycin (Spc, pART27) for *E. coli* strains DH5α or Rosetta (Novagen) or 20 µg/ml rifampicin (Rif) and 50 µg/ml Km, or 250 µg/ml Spc for Agrobacterium strain LBA1115. The constructs pSDM6008 (pET16H:TCH3), pSDM6004 (pGEX:PID) and pSDM6005 (pBluescript SK-PID) were described previously (Benjamins et al., 2003). Primers used in this study are listed in Table 1. To obtain a plasmid encoding the GST tagged first 100 amino acids of PID, the *Sal*I-*Sac*I (blunted) fragment from pSDM6005 was cloned into the *Xho*I and *Hin*dIII (blunted) sites of pGEX-KG (Guan and Dixon, 1991). Fragments encoding the PID catalytic domain (aa 75-398) and the C-terminal part of PID (aa 339-438) were obtained by PCR amplification using the primer pairs PID PK CaD F - PID PK CaD R and PID PK CT F - PID PK CT R, respectively and cloned into pGEX-KG using *Xho*I-*Hin*dIII (blunted) and *Eco*RI-*Hin*dIII (blunted), respectively. To overexpress *TCH3* in *Arabidopsis thaliana*, its complete coding region was cloned from pSDM6008 as a *Bam*HI fragment into pART7 and the expression cassette was inserted as a *Not*I fragment into the pART27 binary vector. To construct *35Spro:TCH3:YFP*, *35Spro:PID:YFP* and *35Spro:PID:CFP,* the coding regions were amplified by PCR from pSDM6008 and pSDM6004 with respectively primers TCH3 attB F1 and TCH3 attB R1, and PID attB F1 and PID attB R1 and the resulting PCR fragments were recombined into pDONOR207 (BP reaction) and subsequently into pART7-derived destination vectors (LR reaction), containing either the *CFP* (PID) or the *YFP* (TCH3 and PID) coding region in frame with the Gateway cassette (Invitrogen). The *35Spro:PID:YFP* expression cassette was inserted as a *Not*I fragment into the pGreenII0179 binary vector.

In vitro *pull-down*

E. coli strain Rosetta (Novagen) was transformed with pSDM6008, pSDM6004, pGEX-PIDaa2-103, pGEX-PIDaa75-398 and pGEX-PIDaa339-438. Single colonies were picked and grown overnight (o/n) at 37^{o}C in 5 ml liquid LC medium containing Cb, 15 µg/ml Km and 34 µg/ml Chloramphenicol (Cam). The o/n culture was diluted 1/20 in 100 ml of fresh LC medium containing Cb and Cam and grown at 37^{o}C until an OD_{600} of 0.8. The cultures were induced with 1 mM IPTG for 4 h and bacteria were harvested by centrifugation and frozen. For GST-tagged PID, frozen bacterial pellets were resuspended in 5 ml Extraction Buffer (EB: 20 mM Tris pH 7.5, 500 mM NaCl, 5 mM EDTA, 1 mM EGTA, 1 mM DTT, 0.2 % Triton X-100, 0.05 % Tween-20) supplemented with 0.1 mM Phenylmethanesulfonylfluoride (PMSF), 0.5 µg/ml Leupeptin and 5 µg/ml Trypsin Inhibitor and incubated on ice for 5 min. After sonication for 2 min, the mixtures were

centrifuged at 10000 g for 15 min at 4°C. Supernatants were added to 500 µl of pre-equilibrated 50 % Glutathione sepharose 4B beads (Amersham-Pharmacia) and incubated for 1 h at 4°C. Beads were washed once with 10 ml EB, and twice with 10 ml Washing Buffer 1 (10 mM Tris pH 7.5, 150 mM NaCl, 5 mM EDTA, 1 mM EGTA, 1 mM DTT). Proteins were eluted by incubating beads at room temperature with 2 ml Elution Buffer 1 (50 mM Tris pH 8.0, 10 mM reduced glutathione). Eluates were passed through MicroSpin chromatography columns (BioRad) and concentrated using Vivaspin 6 device 10000 MWCO (Sartorius). For His-tagged TCH3, bacteria pellets were resuspended in Binding Buffer (BB: 20 mM Tris pH 7.5, 500 mM NaCl, 5 mM $MgCl_2$, 2 mM $CaCl_2$, 1 mM DTT, 0.2 % Triton X-100, 0.05 % Tween-20) supplemented with 0.1 mM PMSF, 0.5 µg/ml Leupeptin and 5 µg/ml Trypsin Inhibitor, incubated for 5 min on ice prior to lysis of cells by 2 min sonication. For *in vitro* pull down assays, 2 µg of purified GST-tagged protein was immobilized on Glutathione High Capacity Coated Plates (Sigma). After three washes with BB, 200 µl of total protein extract containing His-tagged TCH3 was added to each well and incubated for 1 h at 4°C, washed once with BB and twice with Washing Buffer 2 (10 mM Tris pH 7.5, 150 mM NaCl, 5 mM $MgCl_2$, 2 mM $CaCl_2$, 1 mM DTT). Protein complexes were eluted with 25 µl of 2x Laemmli sample buffer and boiled. Eluate samples were analyzed by SDS-PAGE (12 % gel). Proteins were blotted on a PDVF membrane (Millipore, USA) and detected using penta-his antibodies (Qiagen) according to the manufacturer's instructions.

Table 1. Primer list

PID PK CaD F	5'TTC-*Xho*I-TTTCGCCTCAT3'
PID PK CaD R	5'GCGCTCAGTTTAGACCTTTGA3'
PID PK CT F	5'TAATGACG-*Eco*RI-TCCGTAACAT3'
PID PK CT R	5'AAGCTCGTTCAAAAGTAATCGAAC3'
TCH3 attB F1	5'GGGGACAAGTTTGTACAAAAAAGCAGGCTTAATGGCGGATAAGCTCACT3'
TCH3 attB R1	5'GGGGACCACTTTGTACAAGAAAGCTGGGTAAGATAACAGCGCTTCGAACA3'
PID attB F1	5'GGGGACAAGTTTGTACAAAAAAGCAGGCTTCAGCATGTTACGAGAATCAGACGGT3'
PID attB R1	5'GGGGACCACTTTGTACAAGAAAGCTGGGTCAAAGTAATCGAACGCCGCTGG3'
PID exon1 F1	5'TCTCTTCCGCCAGGTAAAAA3'
PID exon2 R1	5'CGCAAGACTCGTTGGAAAAG3'
TCH3pr F1	5'AAATGTCCACTCACCCATCC3'
TCH3pr R1	5'GGGAATTCTGAAGATCAGCTTTTGTCG3'
LBaI	5'TGGTTCACGTAGTGGGCCATCG3'
AtROC5 F	5'CGGGAAGGATCGTGATGGA3'
AtROC5 R	5'CCAACCTTCTCGATGGCCT3'
αTUB F	5'CGGAATTCATGAGAGAGATCCTTCATATC3'
αTUB R	5'CCCTCGAGTTAAGTCTCGTACTCCTCTTC3'

The attB recombination sites are underlined.

Phosphorylation assays

His-tagged proteins were purified by immobilized-metal affinity chromatography. Bacterial pellets were resuspended in 2 ml of Lysis Buffer (LB: 25 mM Tris pH 8.0, 500 mM NaCl, 20 mM imidazole, 0.05 % Tween-20, 10 % glycerol) and incubated 5 min on ice. After sonication for 2 min, 100 µl of 20 % Triton X-100 was added and the mixture was incubated 5 min on ice, followed by centrifugation at 10000 g for 15 min at 4°C. The soluble fraction was added with 400 µl of pre-equilibrated 50 % NTA-agarose matrix (Qiagen) and mixed gently for 1.5 h at 4°C. Beads were washed three times with 2 ml of LB, 2 ml of Washing Buffer 3 (25 mM Tris pH 7.5, 500 mM NaCl, 40 mM imidazole, 0.01 % Tween-20, 10 % glycerol), and 2 ml of Wash Buffer 4 (25 mM Tris pH 7.0, 500 mM NaCl, 80 mM imidazole and 10 % glycerol). Elution was performed by incubating the beads on 600 µl Elution Buffer 2 (25 mM Tris pH 7.0, 300 mM NaCl, 300 mM imidazole, 10 % glycerol) for 30 min at 4°C. Samples were analyzed by SDS-PAGE and quantified.

The Pepchip Kinase Slide A (Pepscan) was used for *in vitro* phosphorylation assays for PID in the presence of TCH3. Thirty ng of His:PID, His:TCH3 and His:PBP1 (Chapter 3, this thesis) were mixed with Kinase Mastermix (50 mM HEPES pH 7.4, 20 mM $MgCl_2$, 20 % v/v glycerol, 0.01 mg/ml BSA, 0.01 % v/v Brij-35, 2 mM $CaCl_2$), 10 µM ATP and 300 µCi/ml γ-^{33}P-ATP (specific activity ~ 3000 Ci/mmol, Amersham). Fifty µl of the reaction mix was incubated with the Pepchip Kinase Slide A for 4 h at 30°C in a humid chamber. Slides were washed twice with 2 M NaCl, twice with water and dried for 30 min. Slides were exposed to X-ray film FUJI Super RX for 12 and 24 h.

Arabidopsis lines, plant growth, transformation and protoplast transfections

The *35Spro:PID-21*, *TCH3pro:TCH3:GUS* and *PIDpro:PID:VENUS* lines were described previously (Sistrunk et al., 1994, Benjamins et al., 2001, Michniewicz et al., 2007). Loss-of-function alleles *pid-14* (SALK_049736), *tch3-1* (SALK_056345) and *tch3-2* (SALK_090554) were obtained from NASC (Alonso et al., 2003).

Arabidopsis seeds were surfaced-sterilized by incubation for 15 min in 50 % commercial bleach solution and rinsed four times with sterile water. Seeds were vernalized for 2 to 4 days and germinated at 21°C, 16 h photoperiod and 3000 lux on solid MA medium (Masson and Paszkowski, 1992) supplemented with antibiotics when required. Two- to three-week old plants were transferred to soil and grown in growth room at 21°C, 16 h photoperiod, 70 % relative humidity and 10000 lux.

To screen for the presence of the different T-DNA insertions, the T-DNA-specific LBaI primer was combined in a PCR reaction with the gene-specific PCR primers PID exon1 F1 or PID exon2 R1 for *pid-14* and TCH3pr F1 or TCH3pr R1 for *tch3-1* and *tch3-2*. Sequencing of the junction fragment and Northern blot analysis were used to confirm the insertion position and full knock-out of the loss-of-function alleles.

Arabidopsis thaliana ecotype Columbia wild type (for *35Spro:TCH3*) or the *35Spro:TCH3-2* line (for *35Spro:PID:YFP*) were transformed by a floral dip method as described (Clough and Bent, 1998) using Agrobacterium LBA1115 strain. The T1 transformants were selected on medium supplemented with 50 µg/ml Km for *35Spro:TCH3* or 20 µg/ml hygromycin (Hm) for *35Spro:PID* and with 100 µg/ml timentin to inhibit the Agrobacterium growth. For further analysis, single locus insertion lines were selected by germination on 25 µg/ml Km or 10 µg/ml Hm.

Protoplasts were obtained from *Arabidopsis thaliana* Columbia cell suspension cultures that were propagated as described (Schirawski et al., 2000). Protoplast isolation and PEG-mediated transfections with 10 µg plasmid DNA were performed as initially indicated (Axelos et al., 1992) and adapted by Schirawski and coworkers (Schirawski et al., 2000). To obtain auxin-starved protoplasts, auxin (NAA) was removed from the media during protoplast isolation. Following transfection, the protoplasts were incubated for at least 16 h prior to observation.

Histochemical staining and microscopy

For the Histochemical detection of *GUS* expression, seedlings were fixed in 90 % acetone for 1 h at -20°C, subsequently washed three times in 10 mM EDTA, 100 mM sodium phosphate (pH 7.0), 2 mM $K_3Fe(CN)_6$ and stained for 2 h in 10 mM EDTA, 100 mM sodium phosphate (pH 7.0), 1 mM $K_3Fe(CN)_6$, 1 mM $K_4Fe(CN)_6$ containing 1 mg/ml 5-bromo-4-chloro-3-indolyl-β-D-glucuronic acid, cyclohexylammonium salt (Duchefa). Seedlings were post-fixed in ethanol-acetate (3:1), cleared in 70 % ethanol and stored in 100 mM sodium phosphate (pH 7.0). *GUS* expression patterns in cleared Arabidopsis seedlings were analyzed using a Zeiss Axioplan II microscope with DIC optics. Images were recorded by a ZEISS camera. Arabidopsis lines expressing YFP-fusion proteins were analyzed with a ZEISS Axioplan microscope equipped with a confocal laser scanning unit (MRC1024ES, BioRad, Hercules, CA), using a 40x oil objective. The YFP fluorescence was monitored with a 522-532 nm band pass emission filter (488 nm excitation). All images were recorded using a 3CCD Sony DKC5000 digital camera. For the protoplast experiments, a Leica DM IRBE confocal laser scanning microscope was used with a 63x water objective, digital zoom and 51 % laser intensity. The fluorescence was visualized with an Argon laser for excitation at 514 nm (YFP) and 457 nm (CFP), with 522-532 nm (for the YFP) and 471-481 nm (for the CFP) emission filters. A transmitted light picture was taken for a reference. The images were processed by ImageJ (http://rsb.info.nih.gov/ij/) and assembled in Adobe Photoshop 7.0.

Förster (Fluorescence) Resonance Energy Transfer (FRET)

Protoplasts were prepared and their fluorescence monitored using a Leica confocal microscope as described above. Lambda scanning was done by excitation at 457 nm (donor,

CFP) and by measuring emission at 5 nm intervals from 460 to 585 nm using a RSP465 filter. Of every interval an image was obtained and the intensity of three fixed areas (regions of interest, ROIs) was quantified using the Leica confocal laser scanning software. The intensity of these three ROIs was averaged and normalized. Per sample lambda scanning was performed on three protoplasts and the obtained normalised intensity of all three protoplasts was averaged and used to calculate the standard deviation. The Student's t-test was used to test for significant differences in wavelength specific intensities between the test sample and the negative control. Significantly quenched donor emission wavelength intensity, combined with significantly increased acceptor emission wavelength intensity was considered indicative for protein-protein interaction-dependent FRET. Similar results were obtained for three independent transfections.

RNA extraction and Northern Blots

Total RNA was purified using the RNeasy Plant Mini kit (Qiagen). Subsequent RNA blot analysis was performed as described (Memelink et al., 1994) using 10 µg of total RNA per sample. The following modifications were made: pre-hybridizations and hybridizations were conducted at 65^{o}C using 10 % Dextran sulfate, 1 % SDS, 1 M NaCl, 50 µg/ml of single strand Herring sperm DNA as hybridization mix. The hybridized blots were washed for 20 min at 65^{o}C in 2x SSPE 0.5 % SDS, and for 20 min at 42^{o}C in respectively 0.2x SSPE 0.5 % SDS, 0.1x SSPE 0.5 % SDS and 0.1x SSPE. Blots were exposed to X-ray film FUJI Super RX. The probe for *TCH3* was isolated from pSDM6008 as a *Bam*HI fragment. The probes for *AtROC5*, for *αTubulin* and *PID* were PCR amplified from Col genomic DNA and column purified (Qiagen). Probes were radioactively labeled using a Prime-a-gene kit (Promega).

Biological assays

For the root collapse assay, about 200 seedlings per line were grown in triplicate on vertical plates on MA medium, while the development of the seedling root was monitored and scored each day during 8 days for the collapse of the primary root meristem. For the phenotypic analysis of *pid-14/+ 35Spro:TCH3-1, pid-14/+ 35Spro:TCH3-3*, *pid-14/+ 35Spro:TCH3-4* and *pid-14/+ tch3-2* lines, about 300 seeds were plated in triplicate on MA medium and germinated for one week. The number of dicotyledon seedlings and of seedlings with specific cotyledon defects was counted and the penetrance of the specific phenotypes was calculated based on a 1:3 segregation ratio for *pid/pid* seedlings. For GUS analysis, seeds of *TCH3pro:TCH3:GUS* were grown for 4 days on MA medium, supplemented with 5 µM IAA when indicated. For the subcellular localization of PID in Arabidopsis roots, vertically grown 3 day-old *PIDpro:PID:VENUS* seedlings were treated with 5 µM IAA (in MA medium) with 30 min pre-treatment with a calmodulin inhibitor (0.5 mM Tetracain, Sigma) or calcium channel blocker (1.25 mM Lanthanum, Sigma)

when indicated. Analysis of the subcellular localization was done using the BioRad confocal microscope as described above.

Accession Numbers

The *Arabidopsis* Genome Initiative locus identifiers for the genes mentioned in this chapter are as follows: *PBP1* (At5g54490), *PID* (At2g34650), *TCH3* (At2g41100), *ROC* (At4g38740), *αTubulin* (At5g44340).

Acknowledgments

The authors would like to thank M. Heisler and J. Braam for kindly providing us with the *PIDpro:PID:VENUS* line and the *TCH3pro:TCH3:GUS* line, respectively, J. Braam for sharing her unpublished data on the *tch3-3* allele, Michael Sauer for PIN localization on *TCH3* gain- and loss-of-function mutants, Arnoud van Marion for technical assistance, and Gerda Lamers and Ward de Winter for their help with the microscopy and the tissue culture, respectively. This work was funded through grants from the Research Council for Earth and Life Sciences (C.G-A.: ALW 813.06.004) with financial aid from the Dutch Organization of Scientific Research (NWO).

References

Alonso,J.M., Stepanova,A.N., Leisse,T.J., Kim,C.J., Chen,H., Shinn,P., Stevenson,D.K., Zimmerman,J., Barajas,P., Cheuk,R., Gadrinab,C., Heller,C., Jeske,A., Koesema,E., Meyers,C.C., Parker,H., Prednis,L., Ansari,Y., Choy,N., Deen,H., Geralt,M., Hazari,N., Hom,E., Karnes,M., Mulholland,C., Ndubaku,R., Schmidt,I., Guzman,P., Aguilar-Henonin,L., Schmid,M., Weigel,D., Carter,D.E., Marchand,T., Risseeuw,E., Brogden,D., Zeko,A., Crosby,W.L., Berry,C.C., and Ecker,J.R. (2003). Genome-Wide Insertional Mutagenesis of Arabidopsis thaliana. Science **301**:653-657.

Antosiewicz,D.M., Polisensky,D.H., and Braam,J. (1995). Cellular localization of the Ca2+ binding TCH3 protein of Arabidopsis. Plant J. **8**:623-636.

Axelos,M., Curie,C., Mazzolini,L., Bardet,C., and Lescure,B. (1992). A Protocol for Transient Gene-Expression in Arabidopsis-Thaliana Protoplasts Isolated from Cell-Suspension Cultures. Plant Physiology and Biochemistry **30**:123-128.

Baum,G., Long,J.C., Jenkins,G.I., and Trewavas,A.J. (1999). Stimulation of the blue light phototropic receptor NPH1 causes a transient increase in cytosolic Ca2+. PNAS **96**:13554-13559.

Benjamins,R., Ampudia,C.S., Hooykaas,P.J., and Offringa,R. (2003). PINOID-mediated signaling involves calcium-binding proteins. Plant Physiol **132**:1623-1630.

Benjamins,R., Quint,A., Weijers,D., Hooykaas,P., and Offringa,R. (2001). The PINOID protein kinase regulates organ development in Arabidopsis by enhancing polar auxin transport. Development **128**:4057-4067.

Bennett,S.R.M., Alvarez,J., Bossinger,G., and Smyth,D.R. (1995). Morphogenesis in Pinoid Mutants of Arabidopsis-Thaliana. Plant Journal **8**:505-520.

Bouché,N., Yellin,A., Snedden,W.A., and Fromm,H. (2005). PLANT-SPECIFIC CALMODULIN-BINDING PROTEINS. Annual Review of Plant Biology **56**:435-466.

Braam,J. and Davis,R.W. (1990). Rain-, wind-, and touch-induced expression of calmodulin and calmodulin-related genes in Arabidopsis. Cell **60**:357-364.

Cheng,S.H., Willmann,M.R., Chen,H.C., and Sheen,J. (2002). Calcium signaling through protein kinases. The Arabidopsis calcium-dependent protein kinase gene family. Plant Physiol **129**:469-485.

Christensen,S.K., Dagenais,N., Chory,J., and Weigel,D. (2000). Regulation of auxin response by the protein kinase PINOID. Cell **100**:469-478.

Clough,S.J. and Bent,A.F. (1998). Floral dip: a simplified method for Agrobacterium-mediated transformation of Arabidopsis thaliana. The Plant Journal **16**:735-743.

Corbálan-Garcia,S., Guerrero-Valero,M., Marin-Vicente,C., and Gomez-Fernández,J.C. (2007). The C2 domains of classical/conventional PKCs are specific PtdIns(4,5)P(2)-sensing domains. Biochem.Soc.Trans. **35**:1046-1048.

Darwin,C. (1880). *The Power of Movement in Plants*. London: John Murray.

Dela Fuente,R.K. and Leopold,A.C. (1973). A Role for Calcium in Auxin Transport. Plant Physiol **51**:845-847.

Esmon,C.A., Tinsley,A.G., Ljung,K., Sandberg,G., Hearne,L.B., and Liscum,E. (2006). A gradient of auxin and auxin-dependent transcription precedes tropic growth responses. PNAS **103**:236-241.

Felle,H. (1988). Auxin causes oscillations of cytosolic free calcium and pH in Zea mays coleoptiles. Planta **V174**:495-499.

Friml,J., Yang,X., Michniewicz,M., Weijers,D., Quint,A., Tietz,O., Benjamins,R., Ouwerkerk,P.B.F., Ljung,K., Sandberg,G., Hooykaas,P.J.J., Palme,K., and Offringa,R. (2004). A PINOID-dependent binary switch in apical-basal PIN polar targeting directs auxin efflux. Science **306**:862-865.

Friml,J., Vieten,A., Sauer,M., Weijers,D., Schwarz,H., Hamann,T., Offringa,R., and Jurgens,G. (2003). Efflux-dependent auxin gradients establish the apical-basal axis of Arabidopsis. Nature **426**:147-153.

Friml,J., Wisniewska,J., Benková,E., Mendgen,K., and Palme,K. (2002). Lateral relocation of auxin efflux regulator PIN3 mediates tropism in Arabidopsis. Nature **415**:806-809.

Galván-Ampudia,C.S. and Offringa,R. (2007). Plant evolution: AGC kinases tell the auxin tale. Trends Plant Sci. **12**: 541-547.

Gehring,C.A., Irving,H.R., and Parish,R.W. (1990a). Effects of auxin and abscisic acid on cytosolic calcium and pH in plant cells. Proc.Natl.Acad.Sci.U.S.A **87**:9645-9649.

Gehring,C.A., Williams,D.A., Cody,S.H., and Parish,R.W. (1990b). Phototropism and geotropism in maize coleoptiles are spatially correlated with increases in cytosolic free calcium. Nature **345**:528-530.

Guan,K.L. and Dixon,J.E. (1991). Eukaryotic Proteins Expressed in Escherichia-Coli - An Improved Thrombin Cleavage and Purification Procedure of Fusion Proteins with Glutathione-S-Transferase. Analytical Biochemistry **192**:262-267.

Harada,A., Sakai,T., and Okada,K. (2003). Phot1 and phot2 mediate blue light-induced transient increases in cytosolic Ca2+ differently in Arabidopsis leaves. Proc.Natl.Acad.Sci.U.S.A **100**:8583-8588.

Lee,J.S. and Evans,M.L. (1985). Polar transport of auxin across gravistimulated roots of maize and its enhancement by calcium. Plant Physiol **77**:824-827.

Lee,S.H. and Cho,H.T. (2006). PINOID Positively Regulates Auxin Efflux in Arabidopsis Root Hair Cells and Tobacco Cells. Plant Cell **18**:1604-1616.

Luan,S., Kudla,J., Rodriguez-Concepcion,M., Yalovsky,S., and Gruissem,W. (2002). Calmodulins and calcineurin B-like proteins: calcium sensors for specific signal response coupling in plants. Plant Cell **14 Suppl**:S389-S400.

Masson,J. and Paszkowski,J. (1992). The Culture Response of Arabidopsis-Thaliana Protoplasts Is Determined by the Growth-Conditions of Donor Plants. Plant Journal **2**:829-833.

McCormack,E. and Braam,J. (2003). Calmodulins and related potential calcium sensors of Arabidopsis. New Phytologist **159**:585-598.

Memelink,J., Swords,K.M.M., Staehelin,L.A., and Hoge,J.H.C. (1994) Southern, Northern and Western blot analysis. In Plant Molecular Biology Manuel, (Dordrecht, NL: Kluwer Academic Publishers).

Michniewicz,M., Zago,M.K., Abas,L., Weijers,D., Schweighofer,A., Meskiene,I., Heisler,M.G., Ohno,C., Huang,F., Weigel,D., Meyerowitz,E.M., Luschnig,C., Offringa,R., and Friml,J. (2007). Phosphatase 2A and PID kinase activities antagonistically mediate PIN phosphorylation and apical/basal targeting in *Arabidopsis*. Cell **130**:1044-1056.

Morris,D.A., Friml,J., and Zazimalova,E. (2004) The functioning of hormones in plant growth and development, the transport of auxins. In Plant hormones: Biosynthesis, signal transduction, action!, kluwer Academic Publishers, Dordrecht, NL), pp. 437-470.

Muday,G.K. and DeLong,A. (2001). Polar auxin transport: controlling where and how much. Trends Plant Sci. **6**:535-542.

Nakajima,K. and Benfey,P.N. (2002). Signaling in and out: Control of cell division and differentiation in the shoot and root. Plant Cell **14**:S265-S276.

Paciorek,T., Zazimalová,E., Ruthardt,N., Petrášek,J., Stierhof,Y.D., Kleine-Vehn,J., Morris,D.A., Emans,N., Jürgens,G., Geldner,N., and Friml,J. (2005). Auxin inhibits endocytosis and promotes its own efflux from cells. Nature **435**:1251-1256.

Petrášek,J., Mravec,J., Bouchard,R., Blakeslee,J.J., Abas,M., Seifertová,D., Wisniewska,J., Tadele,Z., Kubes,M., Covanová,M., Dhonukshe,P., Skupa,P., Benková,E., Perry,L., Krecek,P., Lee,O.R., Fink,G.R., Geisler,M., Murphy,A.S., Luschnig,C., Zazimalová,E., and Friml,J. (2006). PIN Proteins Perform a Rate-Limiting Function in Cellular Auxin Efflux. Science **312**:914-918.

Reinhardt,D., Mandel,T., and Kuhlemeier,C. (2000). Auxin regulates the initiation and radial position of plant lateral organs. Plant Cell **12**:507-518.

Reinhardt,D., Pesce,E.R., Stieger,P., Mandel,T., Baltensperger,K., Bennett,M., Traas,J., Friml,J., and Kuhlemeier,C. (2003). Regulation of phyllotaxis by polar auxin transport. Nature **426**:255-260.

Sabatini,S., Beis,D., Wolkenfelt,H., Murfett,J., Guilfoyle,T., Malamy,J., Benfey,P., Leyser,O., Bechtold,N., Weisbeek,P., and Scheres,B. (1999). An auxin-dependent distal organizer of pattern and polarity in the Arabidopsis root. Cell **99**:463-472.

Sambrook,J., Fritsch F., and Maniatis,T. (1989) Molecular cloning - A laboratory Manual. C.Nolan, ed Cold Spring Harbor Laboratory press, NY, USA).

Sanders,D., Pelloux,J., Brownlee,C., and Harper,J.F. (2002). Calcium at the crossroads of signaling. Plant Cell **14 Suppl**:S401-S417.

Sauer,M., Balla,J., Luschnig,C., Wisniewska,J., Reinöhl,V., Friml,J., and Benková,E. (2006). Canalization of auxin flow by Aux/IAA-ARF-dependent feedback regulation of PIN polarity. Genes Dev. **20**:2902-2911.

Schirawski,J., Planchais,S., and Haenni,A.L. (2000). An improved protocol for the preparation of protoplasts from an established Arabidopsis thaliana cell suspension culture and infection with RNA of turnip yellow mosaic tymovirus: a simple and reliable method. Journal of Virological Methods **86**:85-94.

Shishova,M. and Lindberg,S. (2004). Auxin induces an increase of Ca2+ concentration in the cytosol of wheat leaf protoplasts. J Plant Physiol **161**:937-945.

Siegel,R.M., Chan,F.K., Zacharias,D.A., Swofford,R., Holmes,K.L., Tsien,R.Y., and Lenardo,M.J. (2000). Measurement of molecular interactions in living cells by fluorescence resonance energy transfer between variants of the green fluorescent protein. Sci STKE. **2000**:L1.

Sistrunk,M.L., Antosiewicz,D.M., Purugganan,M.M., and Braam,J. (1994). Arabidopsis TCH3 encodes a novel Ca2+ binding protein and shows environmentally induced and tissue-specific regulation. Plant Cell **6**:1553-1565.

Snedden,W.A. and Fromm,H. (2001). Calmodulin as a versatile calcium signal transducer in plants. New Phytologist **151**:35-66.

Strynadka,N.C.J. and James,M.N.G. (1989). Crystal Structures of the Helix-Loop-Helix Calcium-Binding Proteins. Annual Review of Biochemistry **58**:951-999.

Travé,G., Lacombe,P.J., Pfuhl,M., Saraste,M., and Pastore,A. (1995). Molecular mechanism of the calcium-induced conformational change in the spectrin EF-hands. EMBO J. **14**:4922-4931.

Weijers,D. and Jurgens,G. (2005). Auxin and embryo axis formation: the ends in sight? Current Opinion in Plant Biology **8**:32-37.

Wisniewska,J., Xu,J., Seifertová,D., Brewer,P.B., Ruzicka,K., Blilou,I., Rouquié,D., Benková,E., Scheres,B., and Friml,J. (2006). Polar PIN Localization Directs Auxin Flow in Plants. Science **312**:883.

Zegzouti,H., Li,W., Lorenz,T.C., Xie,M., Payne,C.T., Smith,K., Glenny,S., Payne,G.S., and Christensen,S.K. (2006). Structural and functional insights into the regulation of Arabidopsis AGC VIIIa kinases. J Biol.Chem. **281**:35520-35530.